Ramp-Compressed Sodium at 480 GPa: A Dense Plasma Electride

D. N. Polsin

Laboratory for Laser Energetics, University of Rochester

The limiting high-pressure behavior of matter suggests that some materials transform into simple dense-packed structures with free-electron metallic behavior; examples include the ultradense solids of planetary cores and the hot plasmas of thermonuclear reactions and stellar interiors. This model breaks down at significant compressions where valence–valence and valence–core electron overlap are responsible for the chemical and electronic properties, bringing quantum behavior to the macroscale and giving rise to exotic phases such as high-temperature superconductors, quantum Hall insulators, and electrides. Sodium is the ideal material to explore such behavior due to its remarkable transformation at just 200 GPa from a free-electron simple metal to a structurally complex transparent electride,[1] where electrons are localized in interstitial positions due to the density-driven quantum mechanical constraints on the electronic wave functions.[2] Studies of high-temperature (>1000-K) electride behavior in the solid, liquid, and plasma phases have largely been limited to theoretical studies with no data on the kinetics of these phase transformations on nanosecond time scales.[3,4] Here we report on measurements of the structural and electronic properties of Na in an unexplored regime, where the nearest Na–Na distance approaches the 3*s* orbital radius. Lasers are used as high-pressure drivers to ramp compress Na up to 480 GPa and ~2000 K. X-ray diffraction measurements at these unprecedented pressures and temperatures reveal that the *hP4* electride phase is stable even in a dense plasma state and on nanosecond time scales. At intermediate pressures (242 to 292 GPa), new complex phases with diffraction peaks unaccounted for by the *hP4* structure are observed. The new phase is not transparent—in striking contrast to static compression studies—but a significant decrease in the conductivity is consistent with a transformation to a high-temperature electride phase. Interactions between core electrons occur in all materials at extreme densities and pressures; the formation and understanding of these novel quantum materials in their transient states are the first steps to a new generation of high-energy-density quantum matter.

Sodium's intriguing high-pressure behavior is evident upon inspection of its phase diagram shown in Fig. 1. Sodium transforms from simple cubic structures to at least seven complex, low-symmetry phases near the minimum of the melting curve (blue circles and blue curves) at 118 GPa and room temperature.[5,6] At 147 GPa, it transforms into an incommensurate host–guest structure—a complex structure consisting of two interpenetrating host and guest structures—as the melting temperature begins to increase.[7,8]

This series of high-pressure phase transformations is associated with remarkable transformations in Na's electronic properties with a transition from a mirrorlike metal at ambient pressure to a dark, nonreflecting *tI19* phase at 147 GPa to a transparent insulator at 200 GPa with a band gap of at least 1.3 eV (Refs. 1 and 9). Guided by first-principles structure searching results, the x-ray diffraction pattern from the transparent phase is a distorted double hexagonal close-packed (dhcp) *hP4* electride structure[1] that, together with the interstitial quasi-atoms form the binary Ni_2In structure, shown in Fig. 1 (structural model).

Simultaneous x-ray diffraction (XRD) and reflectivity measurements were performed on the OMEGA EP laser that ramp compressed Na to nearly 500 GPa (Ref. 10). At 409±15 GPa, the diffraction pattern has four peaks, consistent with the *hP4* phase reported in previous room-temperature static compression experiments by Ma *et al.*,[1] but at higher temperatures and under dynamic compression. We index the four lines as the *hP4* (010), (011), (012), and (110), giving lattice parameters $a = b = 2.75 \pm 0.03$ Å and $c/a = 1.35 \pm 0.02$. Compared to the ideal dhcp lattice, with $c/a = 3.27$ for hard spheres, the *hP4* structure is highly distorted and not close packed because the electride nature of this structure stabilizes a more open structure to accommodate the local-

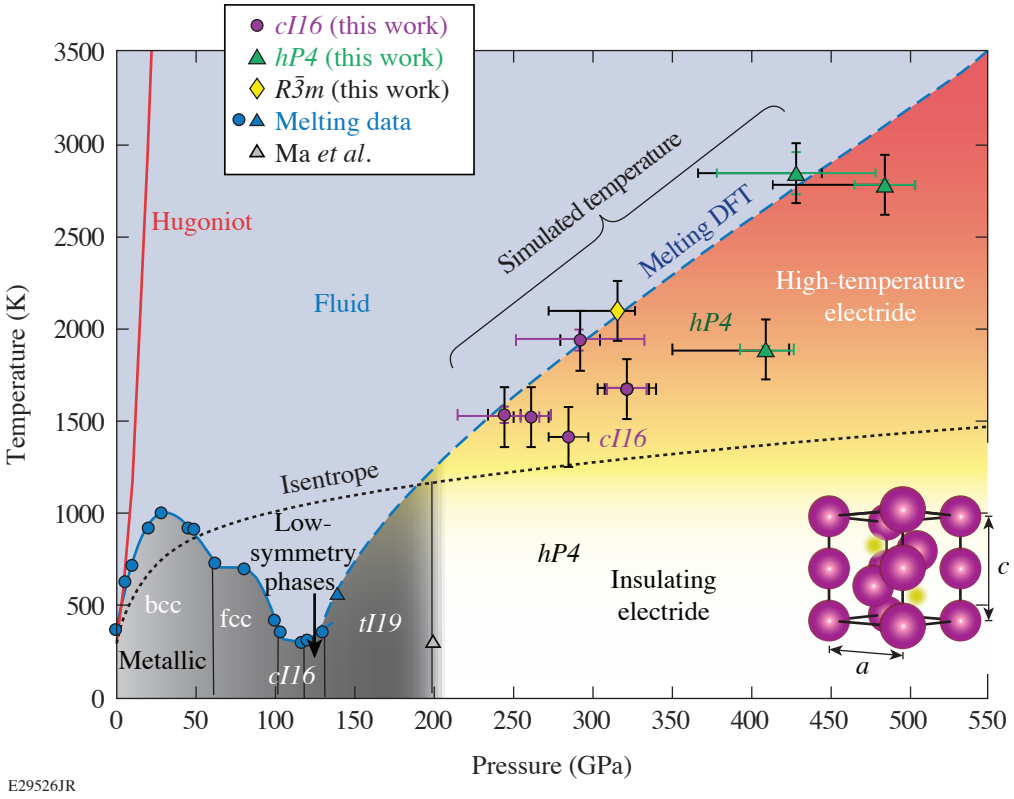

Figure 1

The high-pressure phase diagram of Na based on our laser-driven ramp compression data (purple circles, yellow diamond, and green triangles; black error bars represent systematic and random uncertainties; color "error" bars represent standard deviation in pressure and temperature states within the sample) and previous work from Refs. 1, 5, 6, 8, and 11. The data are compared to the theoretical principal Hugoniot and isentrope. The melting curve data from Refs. 6 and 8 are shown (blue circles and triangle) along with density-functional-theory (DFT) calculations[11] for the melting curve (blue dashed line) above 130 GPa in the *hP4* phase [structural model (bottom right): Na^+ ions (purple), localized electrons (yellow)]. Three different phases of Na, *cI16*, $R\bar{3}m$ and *hP4*, are observed. The temperatures are estimated from hydrodynamics simulations.

ized valence electron charge.[1] Compared to the static compression data (*c*/*a* = 1.46), we observe a decrease in the *c*/*a* ratio with increasing pressure that agrees well with the density functional theory predictions and implies a stronger electron localization.[1]

At pressures between 242 and 292 GPa, the XRD pattern is consistent with a complex *cI16* phase. This is isostructural with the *cI16* phase of sodium near the minimum of the melting curve at lower temperatures and pressures (108 GPa, room temperature)[12] and lithium (40 GPa, 180 K).[13] The *cI16* structure (space group: *I*43*d*, 220) is a body-centered-cubic (bcc) superstructure with 16 atoms on the 16c Wyckoff site. The diffraction pattern has five peaks with a clearly different symmetry than the *hP4* structure, which was observed at these pressures in room-temperature experiments.[1] In one experiment at 315±11 GPa (shot 26479), a diffraction pattern distinct from both *cI16* and *hP4* was observed. The diffraction pattern was compared to those from theoretically predicted structures and other structures observed in alkali metals including *oP8*, *oC16*, *tI4*, and *tI19*, but none were found to match the observed diffraction pattern. A Bravais lattice and space group search[14] suggest a rhombohedral structure (space group: $R\bar{3}m$, 166). This is the same structure observed in As, Sb, and Bi (Ref. 15).

Figure 2(c) shows the average Na reflectivity as a function of time. As seen in both the raw data and the average across all experiments, the Na reflectivity drops to about 23%±4% of its initial value. The temperature–pressure paths of the reflectivity measurements are shown in Fig. 2(d), where hydrocode simulations are used to estimate the temperatures. The reflectivity is tracked through the bcc phase into the stability region of the fluid phase, and at the highest pressures, in the *cI16* phase and approaching the *hP4* phase where it is dark and nonreflective. A threefold drop in electrical conductivity is expected in the low-coordinated

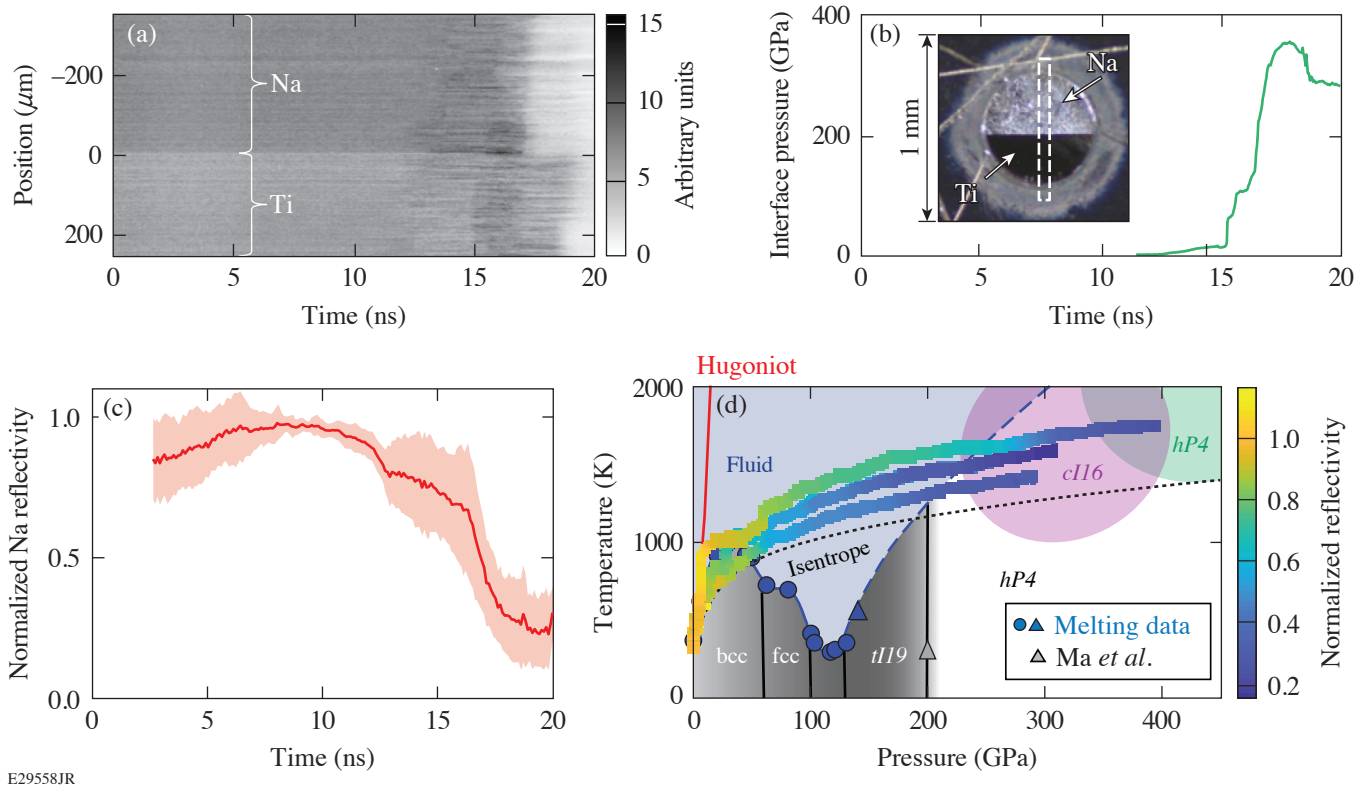

Figure 2

(a) A non-fringing VISAR (velocity interferometer system for any reflector) image for a Na target using a transparent MgO window and containing Ti coatings to detect changes in reflectivity (shot 27971). The non-fringing image is generated by blocking one arm of the VISAR interferometer, and shows no evidence of the pre-imposed striped reflectance pattern with a 150-μm period behind the Na layer. (b) (inset) A microscope image through the high-Z pinhole shows the Na layer (top) and the half-Ti overcoat (bottom) with the VISAR field of view overlaid (dashed box). The interface pressure of the shot shown in (a) shows that the drop in reflectivity is coincident with the increasing pressure. (c) Average (red curve) and standard deviation (red shaded region) of all Na reflectivity data normalized to the Ti reflectivity behind the transparent window. (d) The temperature–pressure phase diagram of Na with the simulated ramp-compression path (multicolor curves) for three reflectivity experiments.

liquid sodium between 40 and 80 GPa (Ref. 16). Similarly in liquid potassium, atomistic simulations predict a continuous transition from a free-electron metal to an electride liquid at pressures corresponding to the melting curve maximum and the onset of electride formation [10 to 20 GPa (K); 30 to 200 GPa (Na)] that manifests as a dip in the reflectivity similar to that observed here.[17] Reduced reflectance is consistently observed in host–guest structures in Na and K at lower pressure.[1,7,18]

Using laser-driven ramp compression, XRD measurements of sevenfold compressed Na are made in a regime where core overlap is thought to stabilize the formation of electride states. The observation of the *hP4* phase at 480 GPa and ~3000 K, which was previously observed to be transparent at 200 GPa and room temperature, implies that electride formation is possible on nanosecond time scales and at higher temperatures. At intermediate pressures, two additional unexpected phases of Na are observed. The reflectivity in both the liquid and solid stability regions is observed to continuously decrease where theory predicts a liquid–liquid phase transition to an electride fluid in alkali metals.[11,17] Interactions between core electrons occur in all materials at extreme densities and pressures, and these results give insight into the structural complexity and core-electron chemistry in Na—the most-striking example of a high-pressure electride.

This material is based upon work supported by the Department of Energy National Nuclear Security Administration under Award Number DE-NA0003856, the University of Rochester, and the New York State Energy Research and Development Authority.

1. Y. Ma *et al.*, Nature **458**, 182 (2009).
2. M.-S. Miao and R. Hoffmann, Account. Chem. Res. **47**, 1311 (2014).
3. X. Dong *et al.*, Nat. Chem. **9**, 440 (2017).
4. J. Dai *et al.*, Phys. Rev. Lett. **109**, 175701 (2012).
5. E. Gregoryanz *et al.*, Science **320**, 1054 (2008).
6. E. Gregoryanz *et al.*, Phys. Rev. Lett. **94**, 185502 (2005).
7. L. F. Lundegaard *et al.*, Phys. Rev. B **79**, 064105 (2009).
8. M. Marqués *et al.*, Phys. Rev. B **83**, 184106 (2011).
9. A. Lazicki *et al.*, Proc. Nat. Acad. Sci. **106**, 6525 (2009).
10. D. D. Meyerhofer *et al.*, J. Phys.: Conf. Ser. **244**, 032010 (2010).
11. R. Paul *et al.*, Phys. Rev. B **102**, 094103 (2020).
12. M. I. McMahon *et al.*, Proc. Nat. Acad. Sci. **104**, 17,297 (2007).
13. M. Hanfland *et al.*, Nature **408**, 174 (2000).
14. B. Toby and R. Dreele, J. Appl. Crystallogr. **46**, 544 (2013).
15. O. Degtyareva, M. I. McMahon, and R. J. Nelmes, High Pressure Res. **24**, 319 (2004).
16. J.-Y. Raty, E. Schwegler, and S. A. Bonev, Nature **449**, 448 (2007).
17. H. Zong *et al.*, Nat. Phys. **17**, 955 (2021).
18. K. Takemura and K. Syassen, Phys. Rev. B **28**, 1193(R) (1983).